Synthesis of Novel Cationic Bleach Activator, N-[4-(N,N,N)-Triethylammoniumchloride- Butanoyl] Butyrolactam, for Cellulose : Optimization and Theoretical Limitations

Pelin Altay (pelinaltay@itu.edu.tr)
Istanbul Teknik Universitesi https://orcid.org/0000-0001-7888-9477
Erol Yildiirm
ODTU: Orta Dogu Teknik Universitesi
Nevin Cigdem Gursoy
Istanbul Teknik Üniversitesi: Istanbul Teknik Universitesi
Peter J. Hauser
North Carolina State University
Ahmed El-Shafei
North Carolina State University

Research Article

Keywords: Cellulose, Peracetic acid, synthesis of bleach activator, N-[4-(N,N,N) triethylammoniumchloride-butanoyl] butyrolactam (TBUCB), low temperature bleaching, DFT calculations, molecular modeling

Posted Date: May 11th, 2021

DOI: https://doi.org/10.21203/rs.3.rs-494060/v1

Abstract

Activated bleach systems have the potential to produce more efficient kinetically potent bleaching systems through increased oxidation rates with reducing energy cost, saving time and, hence, causing less cellulose polymer chains damage or degradation than conventional hot peroxide bleaching. In this study, a novel cationic bleach activator, N-[4-(N,N,N)-triethylammoniumchloride- butanoyl] butyrolactam (TBUCB), was synthesized and applied for hot peroxide bleaching to determine the optimum bleaching conditions and theoretical limitations of TBUCB for low temperature bleaching of cellulose. First principles density functional theory (DFT) calculations were performed to elucidate the reaction mechanism *via* identifying plausible transition state(s) of the nucleophilic attack of perhydroxyl anion (HOO^-) with different carbonyl carbons and identifying the advantages and limitations of TBUCB activator for hydrogen peroxide bleaching for cellulose. The results obtained showed that whiteness index greater than 80 for cellulose can be achieved by using activated H_2O_2-TBUCB bleaching system at lower temperature, providing reduced energy cost while maintaining the integrity of cellulose polymer chains.

Highlights

- The focus of this study is on the chemistry of cellulose, the use of bleach activator as a kinetically potent oxidizing agent for enhancing the degree of whiteness of cellulose.
- A novel cationic bleach activator, N-[4-(N,N,N)-triethylammoniumchloride- butanoyl] butyrolactam (TBUCB), was synthesized and applied for hot peroxide bleaching to determine the optimum bleaching conditions and theoretical limitations of TBUCB for low temperature bleaching of cellulose.
- The reaction mechanism of the bleach activator with cellulose was elucidated and the superior efficiency of the bleach activator while maintaining the integrity of cellulose polymer chains compared to conventional hydrogen peroxide was rationalized.
- DFT calculations elucidated the reaction mechanism, reactivity and peroxide bleaching reaction pathway of the perhydroxyl anion attack at carbonyl group of the butanoyl segment not at the carbonyl carbon of the butyrolactam, which is consistent with the experimental results.
- This study provided key fundamental science principles and suggestions at the molecular level for the design of more efficient bleach activator with higher substantivity for cellulose, thus providing a contribution to the commercialization of this novel, more sustainable and effective cationic bleach activator for cellulose and cellulosic materials.

Introduction

Hydrogen peroxide (H_2O_2) is the most widely used bleaching agent for cellulosic materials to improve the whiteness by eliminating the colored impurities in fibers. It is an environment-friendly oxidizing agent that can be used for hot or cold bleaching processes. Hot peroxide bleaching is often carried out under

extremely high temperatures (>95°C) while cold peroxide bleaching requires extremely long dwell times (>20 hours), resulting in increased fiber damage, energy costs and time consumption. Hydrogen peroxide bleaching is conventionally carried out under alkaline conditions, which requires intensive energy consumption. The dissociation of H_2O_2 into hydrogen and perhydroxyl ions (HOO^-) takes place under alkaline conditions (pH 11–12), therefore strong alkali such as sodium hydroxide and sodium carbonate are added into the bleaching bath to promote the formation of HOO^- anions, which is the active bleaching agent. As the bleaching process is completed, a neutralization process is also required to remove the residual alkali by adding acetic acid, and a large amount of water is also required for washing to remove salt and residual H_2O_2 from the bleached cellulosic fibers. Because dyes can react with oxidizing agents, it is important to remove any remaining H_2O_2, since dyed fabrics even with minor color changes are commercially unacceptable due to strict quality targets. [1-12]

Bleaching at lower temperatures and/or shorter process times can be achieved by addition of a chemical called a bleach activator into an aqueous H_2O_2 solution. Addition of bleach activators into the peroxide bleaching solution is a promising method to lower bleaching temperature, thereby resulting in decreased energy consumption and reduced fiber damage. Bleach activators, with O- or N-bounded acetyl groups, are peracid precursors which are able to react with the strongly nucleophilic perhydroxyl anion to liberate kinetically potent peracid in situ. Peracids enable bleaching at low temperatures because they are stronger oxidizing agents. [8-11, 12-26]

Tetraacetylethylenediamine (TAED), and the sodium salt of nonanoylbenzenesulphonic acid (NOBS) are two activators in widespread commercial use and are widely used in laundry detergent formulations for removal of coloring contaminants from textiles. However, TAED has poor solubility in water and NOBS has a negative charge on its leaving group with long alkyl chain, which leads to low substantivity for cellulose. [10, 15, 19-20]

With the aim of avoiding these limitations, an activated bleaching system using lactam-based cationic bleach activators [**N-[4-(triethylammoniomethyl) benzoyl]lactam chloride (TBLC)]** consisting of aromatic benzoyl chloride was developed and designed by the Procter and Gamble Company. It contains one cationic group (quaternary ammonium cations), which can provide high water solubility and inherent great affinity toward negatively charged cellulosic fibers in aqueous solutions, leading to improved bleach effectiveness. [21-26] Altay et al. synthesized a less expensive, sustainable and more effective aliphatic acyl chloride based cationic bleach activator, N-[4-(N,N,N)-triethylammoniumchloride-butyryl] caprolactam (TBUCC), as compared to aromatic ones. [27]

This study focuses on synthesis, optimization and theoretical limitations of a novel, more sustainable and effective cationic bleach activator, N-[4-(N,N,N)-triethylammoniumchloride- butanoyl] butyrolactam (TBUCB), for cellulose as compared to the aromatic ones reported in previous studies. [13-14, 17-26] Firstly, a novel cationic bleach activator, N-[4-(N,N,N)-triethylammoniumchloride- butanoyl] butyrolactam (TBUCB), was developed and synthesized. γ-butyrolactam, which is a low cost alternative and has higher hydrolytic

stability than ε-caprolactam [28] was used as a leaving group to produce aliphatic peracid with one quaternary ammonium chloride site, N-[4-(N,N,N)-triethylammoniumchloride- butanoyl] butyrolactam (TBUCB). Secondly, experimental study and statistical analysis were carried out to optimize TBUCB- hot peroxide bleaching system at lower temperature for providing reduced energy cost and maintaining the integrity of cellulose polymer chains. Density functional theory (DFT) calculations were performed to determine the limitations of TBUCB at molecular level for cellulose.

Experimental

2.1 Materials

Butyrolactam (99 %), triethylamine (99.5%) and 4-chlorobutanoyl chloride (98%) were purchased from Alfa Aesar (USA). Hydrogen peroxide (35% w/w) was purchased from Alfa Aesar (USA) and peroxide stabilizer (Ruco-Stab OKM) was provided from Rudolf Group (Germany). 100% single jersey knitted cellulosic greige and scoured fabrics were used in bleaching experiments.

2.2 Synthesis of N-[4-(N,N,N)-triethylammoniumchloride- butanoyl] butyrolactam (TBUCB)

N-[4-(N,N,N)-triethylammoniumchloride-butanoyl] butyrolactam (TBUCB) was synthesized using a two-step reaction procedure as previously reported. [27] In the first step, the intermediate was synthesized by the condensation reaction of 4-chlorobutanoyl chloride with butyrolactam to form the corresponding amide (intermediate) and triethylammonium hydrochloride salt as (a byproduct). Butyrolactam (17.2 g, 0.2 mol) was mixed with 0.3 mol triethylamine (30.5 g) in toluene (225 mL). The mixture was refluxed under nitrogen. Subsequently, 4-chlorobutanoyl chloride (28.2 g, 0.2 mol) was dissolved in 75 mL of toluene and added slowly to the solution to obtain the intermediate (4-chlorobutanoyl butyrolactam). The solution was refluxed for 6 h, cooled to room temperature. The reaction mixture was dissolved in tetrahydrofuran (instead of acetonitrile [27]) and the salt as a white powder was separated from the reaction mixture by filtration. The filtrate was rotary evaporated to remove tetrahydrofuran, leaving the pure intermediate.

In the second reaction step, 0.1 mol of 4-chlorobutanoyl butyrolactam (intermediate) was refluxed with triethylamine (0.2 mol) in 150 mL acetonitrile for 4 hours to furnish the cationic bleach activator, **(TBUCB)** (Figure 1) as previously reported. [27] The solution was cooled to room temperature and the solvent evaporated using a rotary evaporator to give the cationic bleach activator, **(TBUCB)**.

2.3 Central composite design and statistical evaluation

Response Surface Methodology (RSM) is a combination of statistical and mathematical methods used to determine the optimum experimental conditions with saving time and cost by reducing the number of experiments. Central composite design (CCD) (orthogonal blocks) was used with TBUCB to establish an optimized TBUCB-activated hot peroxide-cellulose bleaching system since CCD is one of the most favored response surface methodology (RSMs) for process optimization. The experimental design was

performed and multiple factors and their interactions were statistically evaluated using Minitab. [29] The order of experiments was arranged randomly. The significance of the process parameters (independent variables) and their interactions were evaluated by means of analysis of variance (ANOVA) with a 95% confidence level.

In this study, independent variables, which are factors that affect the process, are the concentration of activator, molar ratio of activator:H_2O_2, molar ratio of H_2O_2:NaOH, temperature and time, while the dependent variable, which is the response /outcome that may change as a result of changes in independent variables, is whiteness index (Table 1). Slightly higher molar ratio of alkaline to H_2O_2 was used for activating peroxide in bleaching bath. Five levels of each variable were selected, including 7 at center points, 16 at factorial points, 10 at axial points, giving a total of 33 experiments. Design matrix and bleaching results for TBUCB are given in Table 2.

Table 1. Process parameters and levels of each parameters

Independent variables	**Coded levels and Factor levels**				
	-2	**-1**	**0**	**1**	**2**
(A) Concentration of activator (mmol/L)	15.7 (5 g/L)	22.7 (7.24 g/L)	29.7 (9.47 g/L)	36.7 (11.7 g/L)	43.7 (13.93 g/L)
(B) Molar ratio of activator:H_2O_2	1:2	1:4	1:6	1:8	1:10
(C) Molar ratio of H_2O_2:NaOH	1:1.05	1:1.1	1:1.15	1:1.2	1:1.25
(D) Temp.($^{\circ}$C)	40	50	60	70	80
(E) Time (min.)	30	40	50	60	70

Table 2. Design matrix and CCD response data for TBUCB

Standard order	Run order	A	B	C	D	E	WI
1	30	0	0	0	2	0	79.22
2	25	0	-2	0	0	0	61.42
3	26	0	2	0	0	0	71.37
4	27	0	0	-2	0	0	68.94
5	31	0	0	0	0	-2	69.89
6	29	0	0	0	-2	0	56.45
7	32	0	0	0	0	2	69.53
8	24	2	0	0	0	0	71.11
9	33	0	0	0	0	0	69.10
10	28	0	0	2	0	0	71.55
11	23	-2	0	0	0	0	59.52
12	16	1	1	1	1	1	77.92
13	20	0	0	0	0	0	70.67
14	18	0	0	0	0	0	70.49
15	9	-1	-1	-1	1	-1	66.45
16	19	0	0	0	0	0	69.28
17	4	1	1	-1	-1	1	64.91
18	21	0	0	0	0	0	69.50
19	17	0	0	0	0	0	69.21
20	2	1	-1	-1	-1	-1	57.86
21	13	-1	-1	1	1	1	67.70
22	6	1	-1	1	-1	1	56.92
23	11	-1	1	-1	1	1	69.21
24	5	-1	-1	1	-1	-1	55.60
25	10	1	-1	-1	1	1	70.79
26	3	-1	1	-1	-1	-1	60.42
27	15	-1	1	1	1	-1	68.44

28	8	1	1	1	-1	-1	65.81
29	14	1	-1	1	1	-1	70.66
30	1	-1	-1	-1	-1	1	54.95
31	12	1	1	-1	1	-1	77.53
32	22	0	0	0	0	0	70.17
33	7	-1	1	1	-1	1	60.56

2.4 Bleaching Method*: Hot peroxide bleaching*

Hot peroxide bleaching method was applied to evaluate and optimize the bleaching performance of TBUCB for cellulose. An Ahiba Nuance Infrared Laboratory Dyeing Machine (Datacolor International, USA) was used for the hot peroxide bleaching experiments. The experiments were performed at different concentrations of activator, different molar ratios of H_2O_2 to activator and H_2O_2 to NaOH, different temperature and time as stated in Table 1 to optimize the bleaching recipe for TBUCB. Cellulosic fabric was bleached with hydrogen peroxide with the addition of TBUCB at a liquor-to-goods ratio of 20:1 according to recipe given in Table 1. NaOH (%50 w/w) was used for alkaline pH (11.5-11.9) based on the results of pre-experiments. The bath was heated to target temperature at the rate of 4 ^{0}C/min. 1 g/L stabilizer and 1 g/L wetting agent were kept constant for all experiments. After bleaching, fabric was dried under ambient conditions. Whiteness index (WI) of unbleached cellulosic fabric was 35.77 while the WI of a conventional bleached fabric without TBUCB was 75.77 (Table 3).

Table 3. Recipe of conventional hot peroxide bleaching

Conc. of H_2O_2 (g/L), 35% w:w)	Conc. of NaOH, 50% w:w)	stabilizer	Wetting agent	Temp. (^{o}C)	Time (min.)	WI
6	3	1	1	100	30	75.77

2.5 Evaluation of bleaching performance: *Whiteness measurement*

Bleaching performance of the activator was evaluated by measuring the whiteness index of bleached samples using ultraviolet-calibrated Datacolor Spectraflash SF 600X, under illuminant D65 and 10^0 standard observer, specular included, large area view and UV component included.

2.6 Computational Methods

Density functional theory (DFT) calculations were performed at the B3LYP hybrid functional and 6-311+g(d,p) basis set level in the Gaussian 16 Rev. A.03 software package. [30-33] Geometry optimizations were started from different initial structures to obtain lowest energy geometry. Highest occupied molecular orbitals (HOMO), lowest unoccupied molecular orbitals (LUMO), and electrostatic potential surface (ESP) were calculated and mapped onto the optimized geometry of the TBUCB activator. Atomic charges on the activator were calculated by using ESP fitting scheme of Merz-Singh-Kollman (MK) and atomic dipole moment corrected Hirshfeld atomic charges (ADCH) .[34-36] Fukui reactivity indices for the nucleophilic attack sites on the activator were calculated by using finite difference approximation by using the atomic charges based on the MK charges. [37] The geometry of a transition structure and activation barriers are of key importance in describing the reaction mechanism of hydrogen peroxide anion attack at the most susceptible sites for nucleophilic attacks. Free energy profile for the reaction barrier of the perhydroxyl anion attack to the carbonyl groups were calculated at 70 ˚C. The reaction barrier for the attack to TBUCB is compared with the reaction barrier for TAED activator. The stationary states were determined by vibrational frequencies where transition states were validated as saddle points by only one imaginary frequency. All calculations were performed in water to mimic the experimental conditions by integral equation formalism polarizable continuum model (IEFPCM). [38]

Results And Discussion

3.1 Bleaching performance

The Response Surface Methodology (RSM) based on Central Composite Design (CCD) was used to evaluate and optimize the hot peroxide bleaching process for newly synthesized TBUCB. The Analysis of Variance for WI is given in Table 4.

Coefficients of determination (correlation coefficient) (R^2), ranging from 0% to 100%, indicates the percentage of variation in the response that is explained by the model. The higher the R^2 value, the better the model fits the response data. As can be seen from Table 4, the model is adequate to provide an accurate prediction of response function since R^2 > 0.9 and lack of fit P value >0.05. R^2 is found to be as 99.23%, indicating that 99.23% of the response variability can be explained by the model. $R^2$and Adj-R^2values are higher than 0.9, providing a high trend between the experimental and the predicted values.

Concentration of activator (A), molar ratio of activator:H_2O_2 (B) and temperature (D) are found to have significant influence on WI due to the higher F-ratio (178.94, 187.78, 869.35, respectively) and the smaller significance level (P value<0.05). Temperature (D), followed by molar ratio of activator: H_2O_2 (B) and concentration of activator (A), respectively, present the highest statistical relevance since a higher F ratio indicates greater relevance of the corresponding factor. Although all the interactions between the factors were analyzed, the interactions between the concentration of activator (A) and the molar ratio of activator: H_2O_2 (B), between the concentration of activator (A) and the temperature (D), between the molar ratio of activator: H_2O_2 (B) and the temperature (D) were statistically significant. In terms of F value, the

two-way interaction between the concentration of activator (A) and the molar ratio of activator: H_2O_2 (B) is greater than the other two-way interactions (F= 17. 75).

Table 4. Analysis of Variance for WI

Source	DF	Seq SS	Adj SS	Adj MS	F	P
Blocks	1	14.70	14.70	14.702	16.29	0.002
Regression	20	1271.10	1271.10	63.555	70.43	0.000
Linear	5	1117.23	1117.23	223.446	247.63	0.000
A	1	161.46	161.46	161.461	178.94	0.000
B	1	169.44	169.44	169.442	187.78	0.000
C	1	1.88	1.88	1.876	2.08	0.177
D	1	784.44	784.44	784.441	869.35	0.000
E	1	0.01	0.01	0.012	0.01	0.911
Square	5	121.54	121.54	24.308	26.94	0.000
A*A	1	55.88	66.26	66.261	73.43	0.000
B*B	1	39.37	44.30	44.299	49.09	0.000
C*C	1	1.02	1.86	1.862	2.06	0.179
D*D	1	20.86	21.87	21.871	24.24	0.000
E*E	1	4.41	4.41	4.409	4.89	0.049
Interaction	10	32.32	32.32	3.232	3.58	0.024
A*B	1	16.02	16.02	16.020	17.75	0.001
A*C	1	0.07	0.07	0.069	0.08	0.787
A*D	1	7.74	7.74	7.742	8.58	0.014
A*E	1	0.50	0.50	0.501	0.55	0.472
B*C	1	0.00	0.00	0.002	0.00	0.965
B*D	1	4.92	4.92	4.917	5.45	0.040
B*E	1	0.02	0.02	0.023	0.03	0.875
C*D	1	0.00	0.00	0.000	0.00	0.998
C*E	1	1.56	1.56	1.556	1.72	0.216
D*E	1	1.49	1.49	1.495	1.66	0.225
Residual Error	11	9.93	9.93	0.902		
Lack-of-Fit	6	7.89	7.89	1.315	3.23	0.109
Pure Error	5	2.03	2.03	0.407		
Total	32	1295.73				

S = 0.949912 PRESS = 138.263
R-Sq = 99.23% R-Sq(pred) = 89.33% R-Sq(adj) = 97.77%

2D contour plots, representing a 3D surface on a two-dimensional plane, illustrate the response function of two factors while keeping all other factors constant for the optimization of process conditions. Figure 2(a)-(j) show the two-way interactions of process parameters on WI while all other parameters are at fixed level. It was observed from Figure 2(a) that a whiteness index higher than 70 was obtained at 9.47 g / L (at 0-level) and higher activator concentrations and at a molar ratio of 1: 6-1: 10 activator: H_2O_2.

It is seen from Figure 2(b) that the maximum WI can be obtained at 11.7 g/L of activator concentration (at 1-level) and the increase in the activator concentration to a certain value (approximately to 12.8 g/L) either at a low or high level of alkali (NaOH) range used in the study causes a decrease in the WI. Figure 2(c) indicates that WI higher than 80 can be achieved between 11.7 g/L and 13.93 g/L of activator concentrations at a temperature of 80 ^{o}C. Similar with the trend of alkali concentration in Figure 2(b), (e) and (h), process time has no significant effect on WI as shown in Figure 2(d) (g) and (j). A whiteness index higher than 75 was obtained at a ratio of 1: 6-1: 10 activator: H_2O_2 at a temperature of about 68 to 80 ° C (Figure 2(f)), indicating that peracid became more active resulting in improved bleaching efficiency.

3.2 Computational Results

Mapped Surface for the LUMO on the TBUCB activator given in Figure3a is localized on the butanoyl and butyrolactam groups, especially on the carbonyl groups. One can expect the attack of perhydroxyl anion should be directed at these groups because they are the most electron deficient sites in the activator structure. HOMO orbital which has low possibility for the nucleophilic attack is mainly on the chloride anion and partly on the ethyl ammonium groups (Figure 3b). ESP surface showed that carbonyl groups on the butanoyl and butyrolactam are the only groups that have both electron rich part, depicted by red color on oxygen which can form a hydrogen bond with perhydroxyl anion, in addition to the electron deficient carbonyl carbon depicted by blue color which can undergo nucleophilic attack by peroxide anion, perhydroxyl (Figure 3b). Although there are two carbonyl groups, only the carbonyl carbon of butanoyl is the one that can lead to the formation of peracid (Figure 3c). Atomic charges on the carbon atoms were compared by two different methods to determine which one will be preferred for the anion attack. Both ESP charges based on the electrostatic potential fitting method and charges based on the partitioning of the molecular electron density showed higher positive charge on the carbon atom of the butanoyl carbonyl (Figure 3d-e), which is the main driving force for the initial diffusion and attack by perhydroxyl anion. At last, Fukui reactivity indices for the nucleophilic attack were compared for the two carbonyl carbons, which showed higher potential of the cationic bleach activation to undergo nucleophilic attack by peroxide anion at butanoyl carbonyl carbon rather than butyrolactam carbonyl carbon (Figure 3f). Fukui reactivity indices based on different atomic charge calculation methods gave similar results.

Reactions were found to follow two step mechanisms, which are perhydroxyl anion attack at the carbonyl carbon and the peracid formation. Transition state characterized by the single imaginary frequency was calculated for the perhydroxy anion attack at the TBUCB and free energy profile is given in Figure 4a. Reaction barrier for the perhydroxyl anion attack at the carbonyl carbon calculated by using sum of electronic and thermal free energies at 70˚C was determined as 12.55 kcal/mol under water solvation effect. This activation barrier was compared with the TAED activation barrier, and it was determined that perhydroxyl anion attack has lower reaction barrier for TBUCB determined as 13.72 kcal/mol in addition to the higher solubility than TAED (Figure 4b). There is an interaction between carbonyl carbon and perhydroxyl anion as well as a hydrogen bond formation between the oxygen of the carbonyl and perhydroxyl hydrogen in the transition state. This confirms the importance of initial hydrogen-bonding through these interactions that leads to the nucleophilic attack. Although carbonyl carbon that is part of the butyrolactam has a partial positive charge as a potential site for nucleophic attack, no transition states for perhydroxyl anion attack at the carbonyl carbon of butyrolactam ring was found, which confirms that there is no reaction happening inside ring, which led to the conclusion that the carbonyl group of butyrolactam is not reactive towards perhydroxyl anion attack to form any peracid. The bond distance between carbonyl carbon of butanoyl and the nitrogen atom of butyrolactam significantly increased after perhydroxyl bonding, followed by bond dissociation and peracid formation in the second step of the reaction. The perhydroxyl anion attack in the first step is the rate determining step, and dissociation of peracid for TBUCB and TAED in the second step occurs with a lower energy barrier at 7.88

and 4.58 kcal/mol, respectively. Imaginary frequencies and cartesian coordinates of atoms for the transition states are given in the Supporting Information.

The main limitation of TBUCB is the conformational freedom due to the alkyl group in butanoyl group. Results showed that positively charged triethyl ammonium group is attracted toward the more negative oxygen atoms of either butanoyl (Figure 5a and 5c) or butyrolactam (Figure 5b and 5d) groups, resulting in a bent conformation with decreased reactivity, thereby preventing more peracid formation. In addition, steric interactions cause a barrier for perhydroxyl ion to reach to the activator in bleaching bath for peracid formation. Although all *trans* coplanar conformation is the lowest energy structure, *gauche1* (Figure 5a and 5c) and *gauche2* (Figure 5b and 5d) conformers of these alkyl groups were easily obtained with less than 2 kcal/mol energy difference. The closest distance between ethylammonium hydrogens and butanoyl oxygen which was 4.51 Å in the lowest energy structure, decreased to 2.51 Å in *gauche1* structure. The closest distance between ethylammonium hydrogens and butyrolactam oxygen which was 6.02 Å in the lowest energy structure, decreased to 4.51 Å in *gauche2* structure (Figure c-d).

When phenyl is used in the molecule structure (Figure 5e) similar with the structure reported as N-[4-(triethylammoniomethyl)benzoyl]caprolactam chloride (TBCC) in the literature [Hou, Zhang & Zhou, 2010; Xu, Hinks, & Shamey, 2010a; Luo et al., 2015], the interaction between triethyl ammonium and the oxygen atoms of the carbonyl group decreased since the butanoyl segment can adopt different conformations while the phenyl group is highly rigid. However, the reactivity of the butanoyl carbonyl towards nucleophilic attacks significantly decreased by phenyl substitution. Alkene modification can be a better alternative to achieve more rigid structure to prevent folding of this aliphatic chain in the future studies (Figure 5f). Unlike butanoyl group, rigid conformations of alkene group hinder coplanar structure from intramolecular interaction and keep the plane of molecule parallel to cellulose surface without compromising nucleophilic reactivity. In general, future work of the developments of novel activator should focus on more rigid, linear and coplanar bleach activator/peracid to achieve better substantivity for cellulose, which would mimic the substantivity of direct dyes to cellulose.

Conclusion

This study focuses on optimization and determination of theoretical limitations of hot peroxide bleaching bath in the presence of newly designed, more sustainable and cost-effective cationic bleach activator, N-[4-(N,N,N)-triethylammoniumchloride-butanoyl] butyrolactam (TBUCB) for low temperature bleaching of cellulose.

CCD results indicate that the most important factors on WI are temperature, followed by molar ratio of activator: H_2O_2 and concentration of activator, respectively, based on the results of ANOVA. Maximum whiteness index of 77.53 can be achieved at 11.7 g/L (36.7 mmol) at 1:8 molar ratio of activator: H_2O_2 at 70 ^{o}C, providing reduced energy cost and fiber damage as compared to conventional peroxide bleaching (WI: 75 at 100 ^{0}C) . With the use of this more sustainable and cost-effective bleach activator [27] in bleach bath, bleaching system can be optimized and WI higher than 80 can be achieved using 11.7 g/L up to

about 12.8 g/L activator concentration at 1:8-1:10 molar ratio of activator to H_2O_2 at a temperature of 80 ^oC. DFT calculations validated the structure, reactivity and peroxide bleaching reaction pathway for the perhydroxyl attack at carbonyl group of the butanoyl segment not at the carbonyl carbon of the butyrolactam, which is consistent with the experimental results. All these findings will contribute to the commercialization of this novel, more sustainable and effective cationic bleach activator. Furthermore, this study also provided key fundamental science principles and suggestions at the molecular level for the design of more efficient bleach activator with higher substantivity for cellulose.

Declarations

Conflict of interest/Competing interests

The authors have no conflicts of interest to declare that are relevant to the content of this article.

Availability of data and material

The authors confirm that the data supporting the findings of this study are available within its supplementary material.

Code availability

Not applicable

Ethics approval

Not applicable

Consent to participate

Not applicable

Consent for publication

Not applicable

References

1. Kamakar S (1999) Chemical Technology in the Pre-Treatment Processes of Textiles. 1st Edition, Elsevier Science, ebook ISBN: 9780080539478.
2. Lewin M (1984) Bleaching of cellulosic and synthetic fabrics: In M. Lewin, & S. B.Sello (Eds.), Handbook of fiber science and technology (pp. 175–228), New York:Marcel Dekker, Inc.
3. Wilding M A (1995) Chemistry of the Textiles Industry, first edition, Chapter 2: Whitening of textiles. Blackie Academic & Professional.

4. Perkins WS (1996) Textile Coloration and Finishing. Carolina Academic Press, Durham, NC, USA.
5. Cockett SR, Hilton KA (1955) Basic Chemistry of Textile Preparation. National Trade Press, London.
6. Clark M (2011) Handbook of Textile and Industrial Dyeing: Principles, Processes and Types of Dyes. Elsevier, Woodhead Publishing Series in Textiles. ISSN 2042-0811.
7. Hofmann J, Just G, Pritzkow W, & Schmidt H (1992) Bleaching activators and the mechanism of bleaching activation. Journal für Praktische Chemie/Chemiker- Zeitung 334(4): 293–297.
8. Wang J, Washington NM (2002) Hydrophobic Bleach Systems and Textile Preparation: A Discontinuity in Fabric Care. AATCC Rev 2(6): 21-24.
9. Grime K, Clauss, A (1990) Laundry bleaches and activators. Chem Ind 15, 20: 647-653.
10. Hou A, Zhang X, Zhou Y(2010) Low temperature bleaching of cellulose fabric with (N-[4-triethylammoniomethyl]-benzoyl) caprolactam chloride as novel cationic activator for H_2O_2 Carbohydrate Polymers 82: 618–622.
11. Abdel-Halim ES, Al-Deyab SS (2011) Low temperature bleaching of cotton cellulose using peracetic acid. Carbohydrate Polymers 86: 988–994.
12. Gursoy NC, Lim SH, Hinks D, Hauser P (2004) Evaluating Hydrogen Peroxide Bleaching with Cationic Bleach Activators in a Cold Pad-Batch Process. Textile Res J 74(11): 970-976.
13. Xu C, Hinks D, & Shamey R (2010a) Bleaching cellulosic fibers via pre-sorption of N-[4-(triethylammoniomethyl)-benzoyl]-butyrolactam chloride. Cellulose 17(4):849–857.
14. Xu C, Shamey R, Hinks D (2010b) Activated peroxide bleaching of regenerated bamboo fiber using a butyrolactam-based cationic bleach activator. Cellulose 17(2):339– 347.
15. Xu C, Long X, Du J, Fu S (2013) A critical reinvestigation of the TAED-activated peroxide system for low-temperature bleaching of cotton. Carbohydr Polym 92(1):249–253.
16. Shao J, Huang Y, Wang Z, Liu J (2010) Cold pad-batch bleaching of cotton fabrics with a TAED/H_2O_2 activating system. Color Technol 126:103–108.
17. Lim SH, Gürsoy NC, Hauser P, Hinks D (2004) Performance of a new cationic bleach activator on a hydrogen peroxide bleaching system. Color Technol 120: 114-118.
18. LongX,XuC,DuJ,FuS(2013)TheTAED/H2O2/NaHCO3systemasanapproachtolow-temperature and near-neutral pH bleaching of cotton. Carbohydr Polym 95(1):107–113.
19. Fei X, Yao J, Du J, Sun C, Xiang Z, & Xu C (2015) Analysis of factors affecting the performance of activated peroxide systems on bleaching of cotton fabric. Cellulose 22(2):1379–1388.
20. Lee JJ, Lim SH, Hauser P, Hinks D (2005) Stability of a novel cationic bleach activator in aqueous solution. Color Technol 121: 37-40.
21. Horvath AT, Horvath AE, Lindstrom T, Wagberg L (2008) Diffusion of cationic polyelectrolytes into cellulosic fibers. Langmuir 24:10797–10806.
22. Zeng H, Tang RC (2015) Application of a novel bleach activator to low temperature bleaching of raw cotton fabrics. The Journal of The Textile Institute 106 (8): 807–813.

23. Luo X, Sui X, Yao J, Fei X, Du J, Sun C, Xiang Z, Xu C, Wang S (2015) Performance modelling of the TBCC-activated peroxide system for low-temperature bleaching of cotton using response surface methodology. Cellulose 22:3491–3499.
24. Cai JY, Evans DJ, Smith SM (2001) Bleaching of natural fibers with TAED and NOBS activated peroxide systems. AATCC Rev 1(12):31–34.
25. Lee b (2011) Review of Bleach Activators for Environmentally Efficient Bleaching of Textiles. Journal of Fiber Bioengineering & Informatics 4(3): 209–219.
26. Hauser PJ, Hinks D, Lee JJ, Lim SH (2007) Cationic bleach activator with enhanced hydrolytic stability. US Patent No: WO2007081724 A2.
27. Altay P, Hauser PJ, Gursoy NC, El-Shafei A (2019) Facile synthesis of a novel, highly effective, more sustainable and cost-effective cationic bleach activator for cotton: N-[4-(N,N,N)-triethylammoniumchloride-butanoyl] Caprolactam. Cellulose 26:2849–2860.
28. Lee JJ, Hinks D, Lim SH, & Hauser P (2010). Hydrolytic stability of a series of lactam-based cationic bleach activators and their impact on cellulose peroxide bleaching. Cellulose 17(3): 671–678.
29. Montgomery DC (2005) Design and Analysis of Experiments. 6th edn., John Wiley and Sons, New York, NY.
30. Stephens PJ., Devlin FJ, Chabalowski CF, Frisch MJJ (1994) Ab Initio Calculation of Vibrational Absorption and Circular Dichroism Spectra Using Density Functional Force Fields. Phys Chem 98: 11623–11627.
31. Becke AD (1993) Density-Functional Thermochemistry. III. The role of exact exchange. Chem Phys 98: 5648–5652. Doi: 10.1063/1.464913
32. Lee C, Yang W, Parr RG (1998) Development of the Colle-Salvetti correlation-energy formula into a functional of the electron density. Phys Rev B 37: 785–789.
33. Frisch MJ, Trucks GW, Schlegel HB, Scuseria GE, Robb MA, Cheeseman JR, Scalmani G, Barone V, Petersson GA, Nakatsuji H, Li X, Caricato M, Marenich AV, Bloino J, Janesko BG, Gomperts R, Mennucci B, Hratchian HP, Ortiz JV, Izmaylov, A F, Sonnenberg JL, Williams-Young D, Ding F, Lipparini F, Egidi F, Goings J, Peng B, Petrone A, Henderson T, Ranasinghe D, Zakrzewski VG, Gao J, Rega N, Zheng G, Liang W, Hada M, Ehara M, Toyota K, Fukuda R, Hasegawa J, Ishida M, Nakajima T, Honda Y, Kitao O, Nakai H, Vreven T, Throssell K, Montgomery JA, Jr Peralta JE, Ogliaro F, Bearpark MJ, Heyd JJ, Brothers EN, Kudin KN, Staroverov VN, Keith TA, Kobayashi R, Normand J, Raghavachari K, Rendell AP, Burant JC, Iyengar SS, Tomasi J, Cossi M, Millam JM, Klene M, Adamo C, Cammi R, Ochterski JW, Martin RL, Morokuma K, Farkas O, Foresman JB, Fox DJ (2016) Gaussian 16, Revision A.03, Gaussian, Inc., Wallingford CT.
34. Besler BH, Merz KM, Jr Kollman P (1990) Atomic charges derived from Semiempirical Methods. J Comput Chem 11: 431–439.
35. Lu T, Chen F (2012) Atomic Dipole Moment Corrected Hirshfeld Population Method. J Theor Comput Chem 11(1):163. https://doi.org/10.1142/S0219633612500113

36. Tian Lu, Feiwu Chen J. (2012) Multiwfn: A multifuctional wavefunction analyzer. Comput Chem 33:580-592.
37. Reed AE, Weinstock RB, Weinhold F (1985) Natural Population Analysis. J Chem Phys 83: 735–746. https://doi.org/10.1063/1.449486
38. J. Tomasi, B. Mennucci, E. Cancès (1999) T**he IEF version of the PCM solvation method: an overview of a new method addressed to study molecular solutes at the QM ab initio level.** J. Mol. Struct THEOCHEM 464: 211-226.

Figures

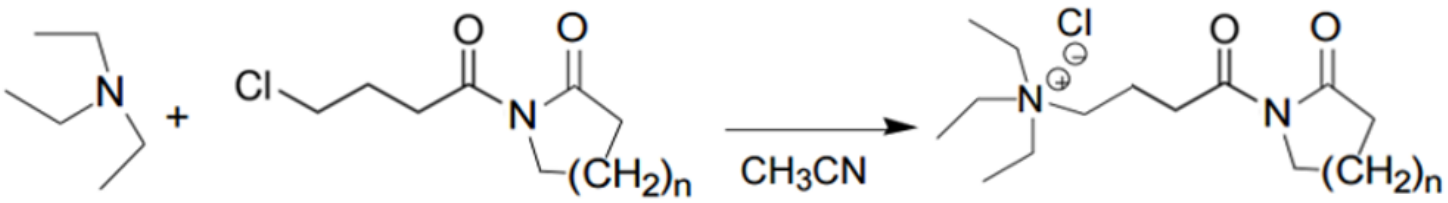

Figure 1

Synthesis of N-[4-(N,N,N)-triethylammoniumchloride- butanoyl] butyrolactam (TBUCB), (n=1) (Mw=290.83)

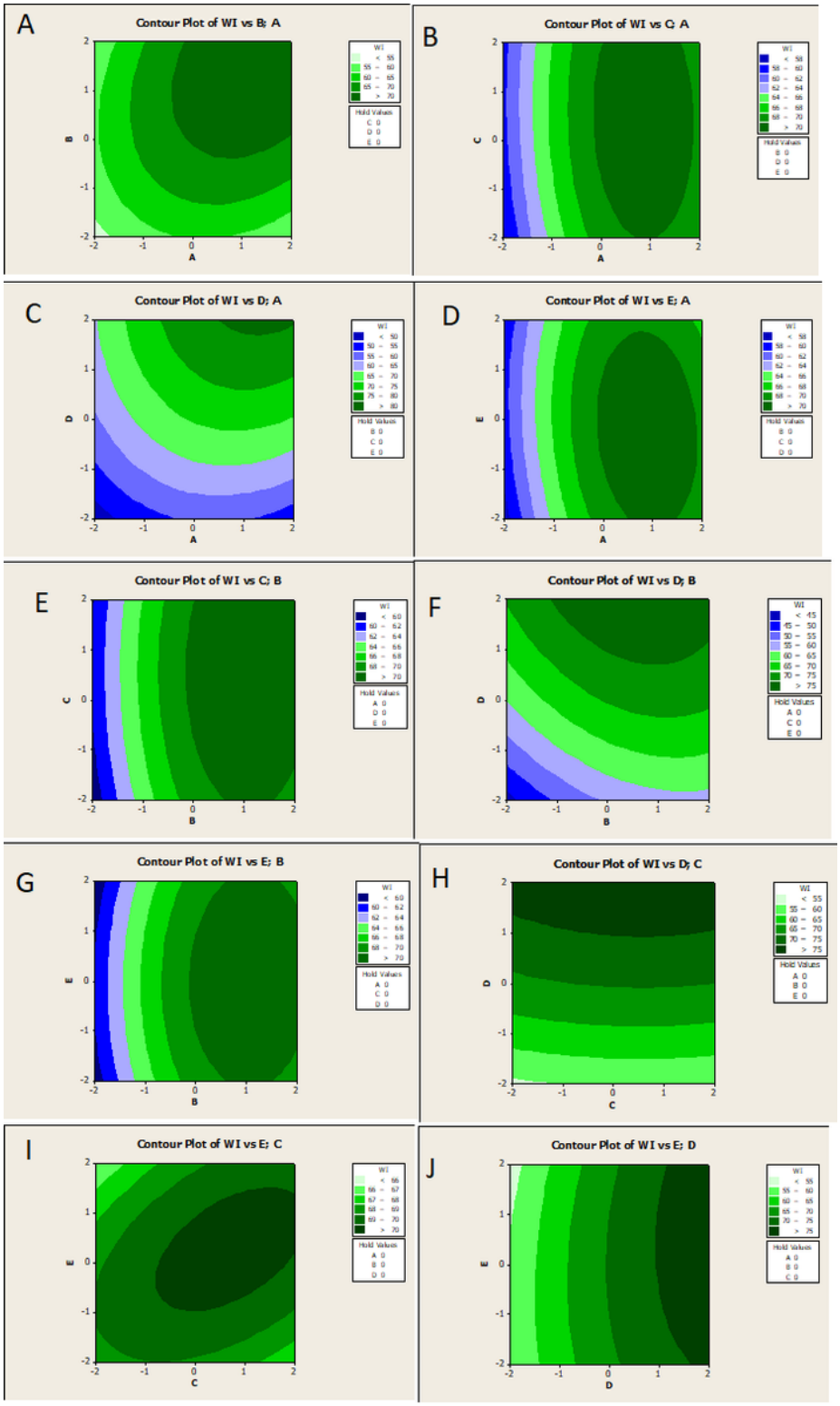

Figure 2

Contour plots showing the effect of independent variables on WI

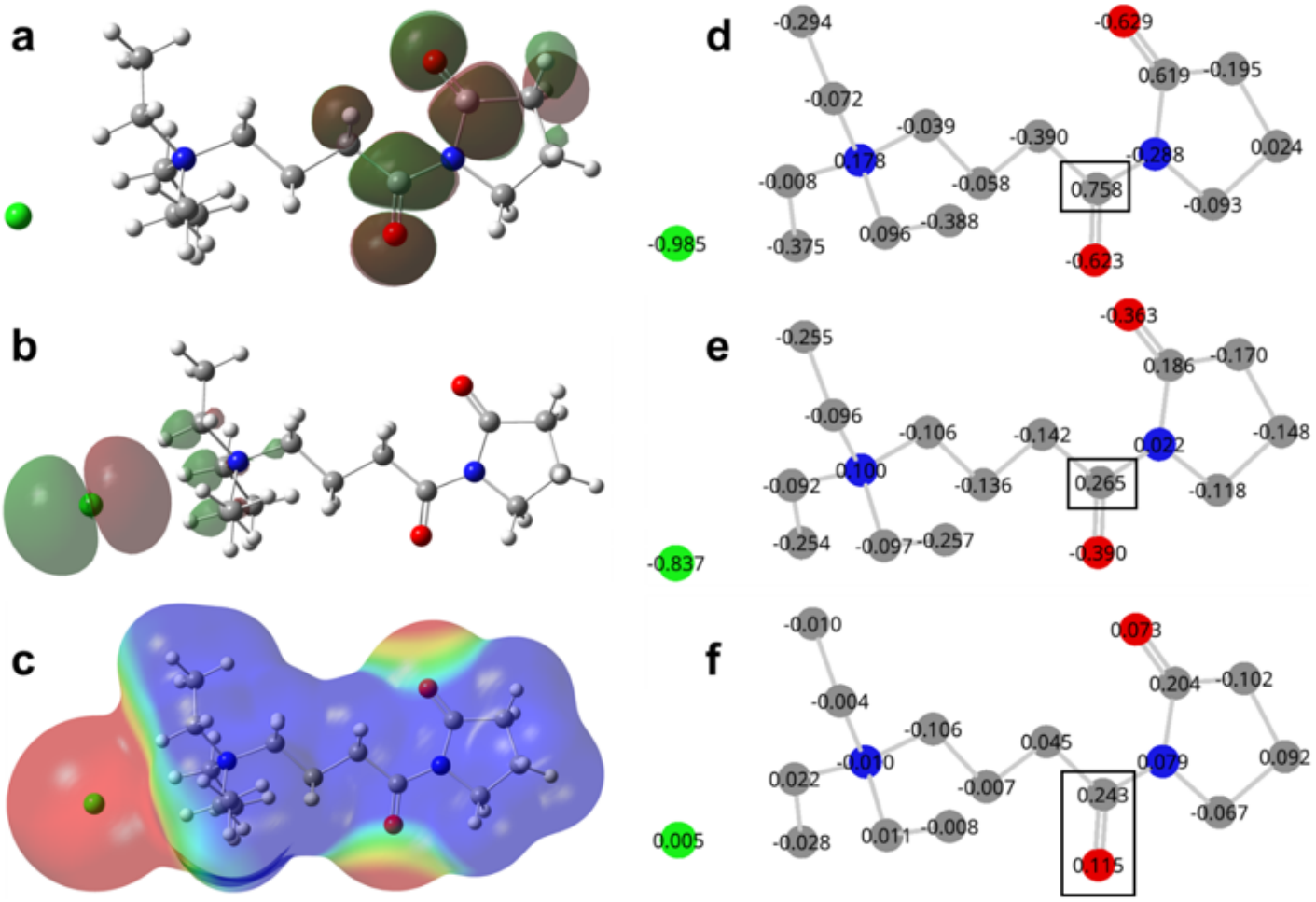

Figure 3

a) LUMO and b) HOMO frontier molecular orbital isosurfaces, c) electrostatic potential (ESP) surface mapped on the optimized geometries. Atomic charges based on the d) electrostatic potential fitting method (MK) and e) atomic dipole moment corrected Hirshfeld (ADHC) population analysis f) Fukui reactivity indices showing the most susceptible sites for nucleophilic attack. Highest charges and reactivity indices are marked.

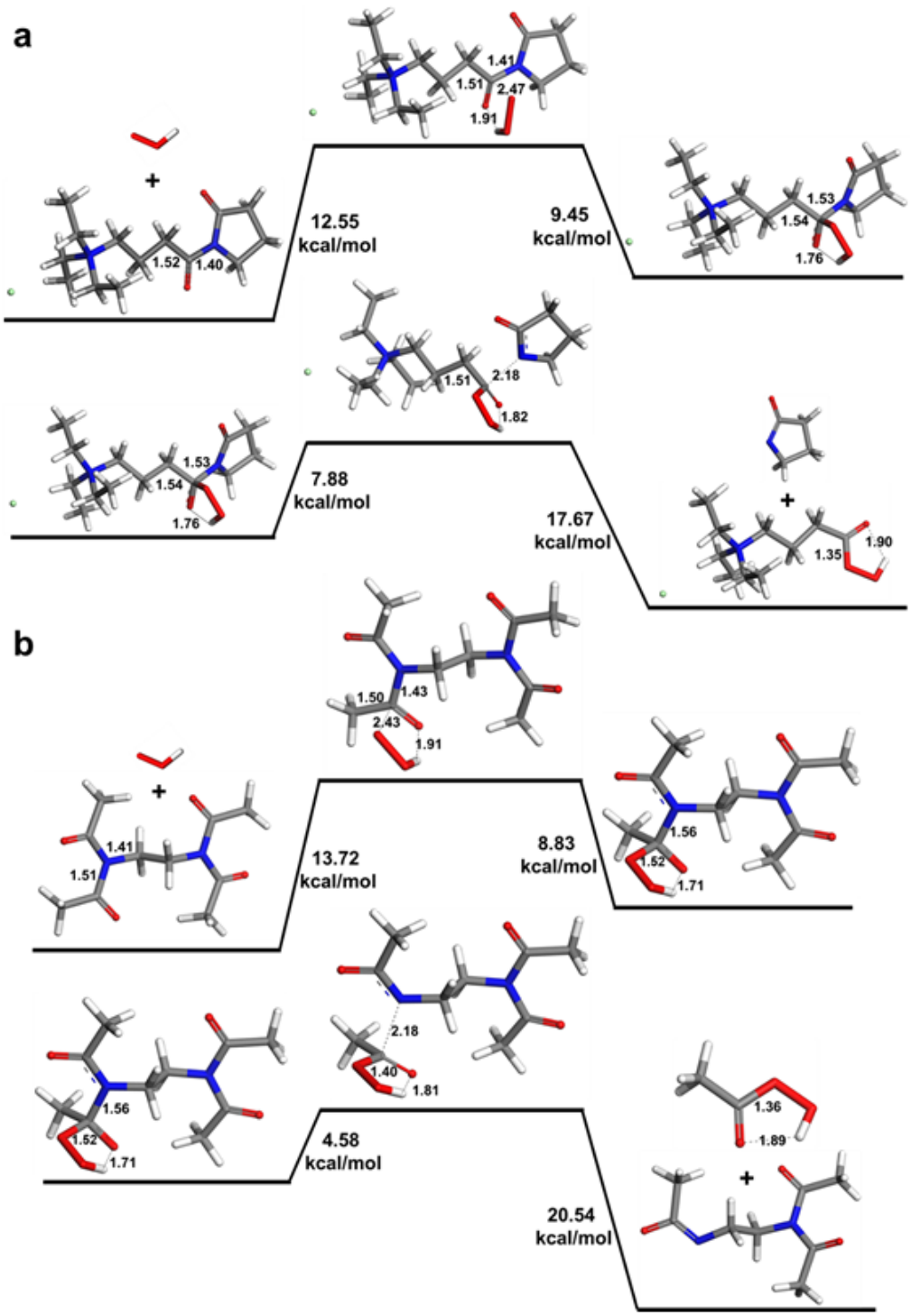

Figure 4

Free energy diagrams of the perhydroxyl anion attack and peracid formation for the a) TBUCB and b) TAED. The relative energies are in kcal/mol and distances are in Å.

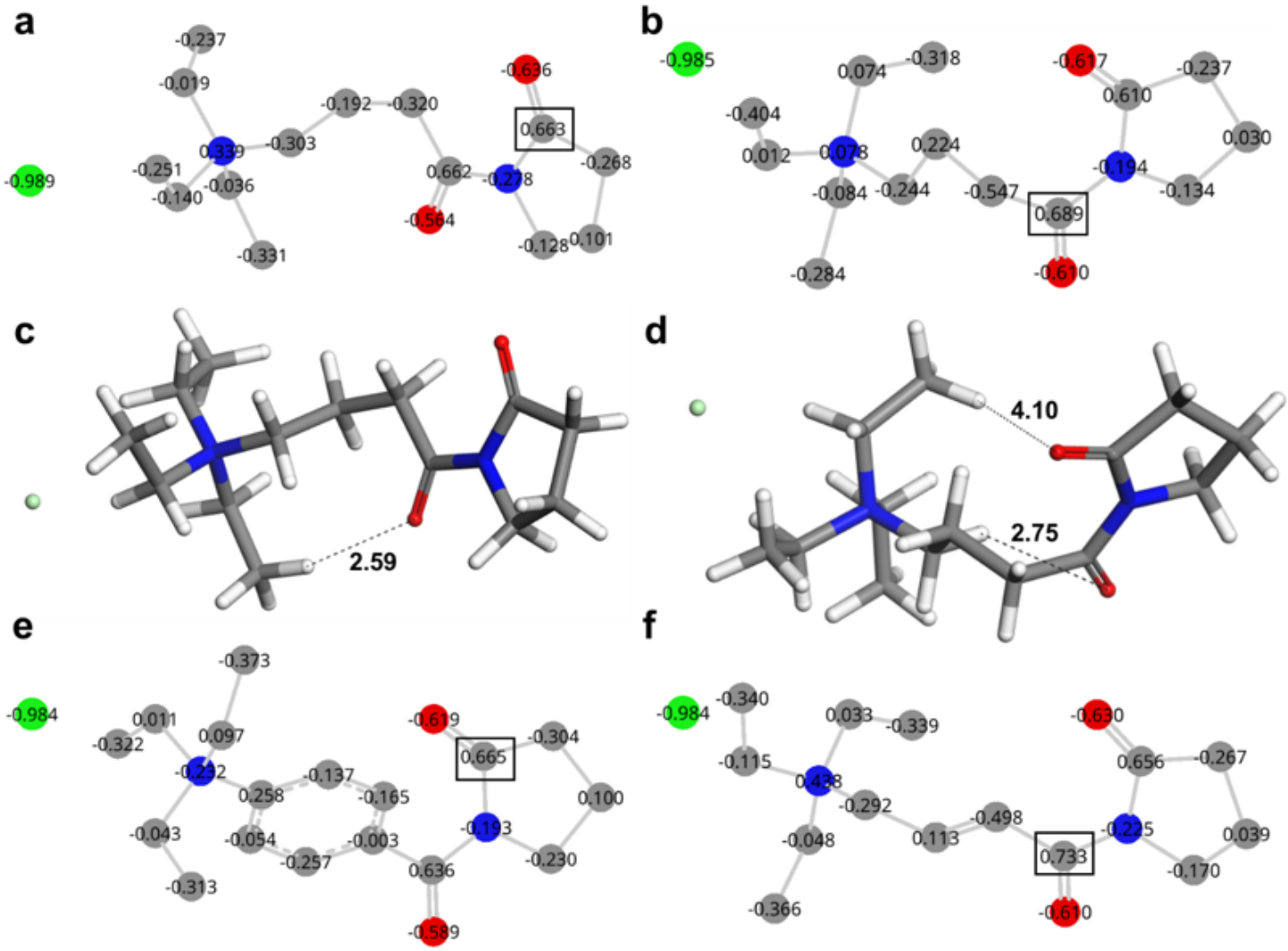

Figure 5

a-c) Non coplanar low energy structures for TBUCB in the gauche1 (a-c) and gauche2 (b-d) conformations, c) alkene modified TBUCB, d) phenyl modified TBUCB. Highest positive charges are marked.

Supplementary Files

This is a list of supplementary files associated with this preprint. Click to download.

- CaptionsfortheSupportingInformation.docx
- Cartesiancoordinatesfortransitionstates.docx
- SI1a.gif
- SI2a.gif
- SI3a.gif
- SI4a.gif